BACKCALCULATION OF PERMANENT DEFORMATION PARAMETERS USING TIME SERIES RUT DATA FROM IN-SERVICE PAVEMENTS IN THE LTPP SPS-1 EXPERIMENT

By

Hassan K. Salama, Ph. D.
Research Associate
email: salamaha@egr.msu.edu

Karim Chatti, Ph.D. (Corresponding Author)
Associate Professor
email: chatti@egr.msu.edu

Syed Waqar Haider, Ph. D.
Research Associate
email: syedwaqa@egr.msu.edu

Department of Civil and Environmental Engineering
Michigan State University
3546 Engineering Building
East Lansing, Michigan 48824
phone: 517-355-6534; fax: 517-432-1827

Prepared for presentation and publication
at the
2006 Annual Meeting of TRB, Washington, D.C.

November 15, 2005

No. of figures = 9x 250 = 2,250 word equivalents
No. of tables = 2 x 250 = 500 word equivalents
Text = 4,737 words
Total = 7,487 words

ABSTRACT
In this paper, time series of rut data from 109 in-service pavement sections in the LTPP, SPS-1 experiment were used to predict the permanent deformation parameters for the VESYS mechanistic-empirical rut model. This was accomplished by matching the rut performance curves versus time for each section using a commercially available iterative solver. To insure uniqueness of each section's PDPs, the transverse surface profiles were used to match the most likely contributions by layer according to the criteria proposed in the NCHRP report 468.

On average, the contribution to the total surface rutting from the various pavement layers was as follows: 57 % from the AC layer, 27 % from the base layer, and 16 % from the subgrade. These results confirm that the contribution to the total rutting from AC and base layers are important and need to be included in any mechanistic-empirical design procedure.

INTRODUCTION

Since rutting is a major failure mode in flexible pavements, researchers have been trying to predict rut depth for future rehabilitation and budget allocation. There are two main approaches for the prediction of rutting: the first approach assumes that most of the rutting results from the subgrade layer only, and is no longer valid based on observations from the field. The second approach considers the rutting contribution from all pavement layers, and is not widely used due to the difficulties of determining the elasto-plastic characteristics of pavement materials. Due to increased tire pressures and new axle configurations as well as observations from the field, researchers began to investigate the rutting contribution from all pavement layers. This approach is also implemented in the new mechanistic-empirical [ME] pavement design guide.

One of the main models related to this approach is the VESYS rutting model that relates the plastic strain to the elastic strain through the permanent deformation parameters (PDPs) μ and α as follows:

$$\varepsilon_p(n) = \mu * \varepsilon_e * n^{-\alpha} \quad (1)$$

The most essential task in using this model is to accurately calculate PDPs (μ and α) for each pavement layer within the pavement system. Several attempts have been made to estimate these parameters; however agreement between studies varies, providing a common but wide range for these parameters. As can be seen in Equation 1, α is an exponent and therefore prediction of rutting is very sensitive to it. In this research, PDPs were backcalculated by matching the rut time series data from the SPS-1 experiment in the LTPP program. Figure 1 shows the locations of SPS-1 sites and the descriptive statistics of the experimental factors. Details regarding the SPS-1 experiment are available elsewhere (*1*).

The most novel aspect of this backcalculation process involved the application of the approach developed in NCHRP 468 (*2*), which uses transverse surface profiles to locate the layer causing most of rutting. Using this process, the most likely solution for these parameters was attained for each pavement section within the SPS-1 experiment– a result that was empirically unattainable from previous approaches.

The main objective of this paper is to present a systematical approach for calibrating a mechanistic-empirical rutting model (VESYS) for flexible pavements using field data from in-service pavements in the SPS-1 experiment.

BACKGROUND

Mechanistic-Empirical rut models

Rutting is a major failure mode for flexible pavements. Two mechanistic modeling approaches have been developed to predict rutting. The first approach is referred to as the subgrade strain model, while the second approach considers permanent deformation within each pavement layer.

The two most widely used equations related to the subgrade strain model are the Asphalt Institute (AI) model (*3*) and the Shell Petroleum model (*4*).

$$N_p = 1.365 \times 10^{-9} \ \varepsilon^{-4.477} \quad \text{(AI)} \quad (2)$$

$$N_p = 6.15 \times 10^{-7} \ \varepsilon^{-4} \quad \text{(Shell)} \quad (3)$$

Where:

N_p = Number of load repetitions to failure

ε_c = Vertical compressive strain at the top of subgrade.

Failure is defined as the development of 13-19 mm (0.5 to 0.75 in) rut depth in the AI model and 13 mm (0.5 in) rut depth in the Shell model. Ullidtz's (*5*) literature review shows that the subgrade strain models (AI and Shell models) are based on unreasonable assumptions, since they only account for subgrade rutting while neglecting upper pavement layer rutting. He also, reported that the subgrade rutting in the AASHO road test was only 9% of the total rutting, while 32% and 59% of the rutting was contributed by the HMA and base/subbase layers, respectively.

Kim (*6*) developed a rutting model which accounts for the total rutting from all pavement layers. However, the model does not separate the contribution from each layer and is limited to using ESALs.

The VESYS rutting model (*7*) was derived so that each term of the equation corresponds to one pavement layer with two unique permanent deformation parameters (α and μ). The form of the model is more applicable for use in mechanistic-empirical design (*8, 9*).

$$\rho_p = h_{AC}\frac{\mu_{AC}}{1\text{-}\alpha_{AC}}\left(\sum_{i=1}^{K}(n_i)^{1-\alpha_{AC}}\left(\varepsilon_{e_i,AC}\right)\right) + h_{base}\frac{\mu_{base}}{1\text{-}\alpha_{base}}\left(\sum_{i=1}^{K}(n_i)^{1-\alpha_{base}}\left(\varepsilon_{e_i,base}\right)\right) + h_{SG}\frac{\mu_{SG}}{1\text{-}\alpha_{SG}}\left(\sum_{i=1}^{K}(n_i)^{1-\alpha_{SG}}\left(\varepsilon_{e_i,SG}\right)\right) \quad (4)$$

Where:

ρ_p = total cumulative rut depth (in the same units as the layer thickness),
i = subscript denoting axle group,
K = number of axle group,
h = layer thickness for AC layer, combined base layer, and subgrade layer, respectively,
n = number of load applications,
ε_e = compression vertical elastic strain at the middle of the layers,
μ = permanent deformation parameter representing the constant of proportionality between plastic and elastic strain, and
α = permanent deformation parameter indicating the rate of change in rutting as the number of load applications increases.

Ali *et al*. (*8*) calibrated the new form of the above model using 61 sections from the Long Term Pavement Performance (LTPP) General Pavement Study 1 (GPS-1) by backcalculating the permanent deformation parameters for each layer. The analysis was based on using the latest rut depth as opposed to time series data. Ali and Tayabji (*9*) also proposed using the transverse profile to backcalculate permanent deformation parameters. However, they reported only one set of values obtained from one LTPP section (see Table 1).

Kenis and Wang (*10*) used Accelerated Pavement Test (APT) performance data to validate and calibrate the two flexible pavement-rutting models used in mechanistic flexible pavement analysis system, VESYS 5. They suggested a wide range of α and μ values for each pavement layer, as shown in Table 1.

The new mechanistic-empirical design procedure developed under NCHRP 1-37A (*12*) provides a rutting model for the AC layer (Equation 5) as well as unbounded layers (Equation 6).

$$\frac{\varepsilon_p}{\varepsilon_r} = 0.0007\beta_{r1}T^{1.734\beta r2}N^{0.3994\beta r3} \quad (5)$$

where:

ε_r = resilient strain
ε_p = plastic strain
T = layer temperature
N = number of load repetitions
β_{r1}, β_{r2}, β_{r3} = field calibration factors

$$\delta_a(N) = \beta_{s1}\varepsilon_v\left(\frac{\varepsilon_0}{\varepsilon_r}\right)e^{-\left(\frac{\rho}{N}\right)^{\beta}}h \quad (6)$$

where:

δ_a = permanent deformation for the layer
N = number of load repetitions
ε_v = average vertical strain
h = thickness of the layer
ε_0,ρ,β = material parameters
ε_r = resilient strain
β_{s1} = field calibration factor

The field calibration factors for these two models are given elsewhere (*12*). A limitation of this model is that it assumes the contribution of different pavement layers to rutting to be constant irrespective of the pavement section.

Contribution of Pavement Layers to Rutting

Rutting is the load-induced permanent deformation of a flexible pavement. According to the magnitude of the load and the relative strength of the pavement layers, permanent deformation can occur in the subgrade, the base, or hot mix asphalt (HMA) layers. Susceptibility of pavement layers to rutting varies according to pavement material properties and climatic conditions. For example, rutting of HMA layers is more common during hot summer seasons than it is during the winter, and permanent deformation is more likely in unbound sub-layers during wet spring seasons. Suitable rehabilitation of existing rutting requires knowledge of the relative contributions of the layers (i.e., subgrade, base, and HMA) to the total permanent deformation in the pavement. There are two main ways to identify the layers primarily responsible for the rutting of a flexible pavement: 1) trenches and 2) transverse surface profile. The rut depth measurements are not precise in the trenched unbounded layers (base, subbase, and subgrade) due to the inconsistency of layer thicknesses and noise caused by individual particles at the surface. Moreover, digging trenches is expensive and difficult to maintain. On the other hand, measuring a transverse surface profile is easier, less hazardous, and far less costly than cutting a transverse trench to examine underlying layers. Therefore, great effort has been made to investigate and analyze the transverse surface profile in order to determine rutting within the pavement layers (*2, 13, and 14*).

Simpson *et al.* (*15*) introduced a technique in which the area under the transverse surface profile can be used to determine whether rutting can be attributed to the effect of heave, or changes in the subgrade, base, or asphalt layer. This technique is based on a linear elastic model to predict the shape of the surface profile. Figure 2 shows transverse profile shapes for various rut mechanisms.

White *et al. (2)* extended Simpson's method using a nonlinear visco-elastic finite element model to predict pavement deformation. The FEM analysis matched Simpson's predictions and, in addition, it was able to separate the effects of the base from those of the HMA layer. Furthermore, trenching data was used to verify the predictions made with transverse surface profiles.

The following equations represent the criteria developed by White, *et al. (2)* to determine the failed layer identity using transverse surface profile data:

$$A = A_p + A_n \tag{7}$$

$$R = \left| \frac{A_p}{A_n} \right| \tag{8}$$

$$C_1 = (-858.21)D + 667.58 \tag{9}$$

$$C_2 = (-1509)D - 287.78 \tag{10}$$

$$C_3 = (-2{,}120.1)D - 407.95 \tag{11}$$

where:

A = total area
A_p = positive area (see Figure 2)
A_n = negative area (see Figure 2)
R = area ratio
C_1 = theoretical average total area for HMA failure, mm^2
C_2 = theoretical average total area for base/subbase failure, mm^2
C_2 = theoretical average total area for subgrade failure, mm^2
D = maximum rut depth, mm (see Figure 2)

Based on the characteristics of a given surface profile and the criteria described above, the following outcomes can be predicted:

(a) Failure will occur in the AC layer if:
$R > 0.05$ and $A > (C_1+C_2)/2$
(b) Failure will occur in the base/subbase layer if:
$R < 0.05$ and $A > (C_2+C_3)/2$

(c) If none of the above criteria are satisfied, that suggests subgrade layer failure.

Figure 3 (a), (b), and (c) shows examples of transverse surface profiles for failed AC, base, and subgrade layers, respectively using the above criteria.

CALIBRATION PROCEDURE

The rutting model form of Ali *et al*.(*8*) is appropriate to predict the individual contributions of pavement layers to total rutting in the context of mechanistic-empirical design; however the calibration of the permanent deformation parameters was not based on time series rut data. Hence, a calibration procedure for this model is suggested in this paper using the LTPP Special Pavement Study-1 (SPS-1) data. This experiment provides rut data for various combinations of layer thickness and base type with fine as well as coarse grained subgrade soils and for different climatic zones (*1*).

Determining the actual values for the PDPs for each pavement layer is the most challenging task to achieve an accurate rutting prediction. The flow chart in Figure 4 shows the process used to predict the values of α and μ from in-service pavements in the SPS-1 experiment. The following details the procedure adopted.

Backcalculation of Pavement Layer Moduli

The initial layer moduli for each SPS-1 pavement section were backcalculated using Falling Weight Deflectometer (FWD) data obtained after the initial construction of the test sections. The MICHBACK computer program was used for this purpose. This was done in order to calculate the vertical compressive strain at the middle of each pavement layer. The process of layer moduli backcalculation yields a variety of possible values, some of which are highly improbable. Therefore, several criteria were used to ensure accurate and reliable backcalculation of pavement layer moduli (*16*).

The FWD test temperature varies with time and space even between point locations within the same section. Therefore, the backcalculated AC modulus was corrected for the standard temperature of 68^{o}F (20^{o}C). The model developed by Park (*17*) was used for this purpose.

Forward Analysis

The VESYS model relates the plastic strain occurring in each pavement layer to the vertical elastic compressive strain in that layer. There are several computer programs available for conducting the forward analysis. In this research, the KENLAYER computer program developed by Huang (*18*) was used to calculate the vertical compressive strain at the middle of each pavement layer, assuming that the mid-depth strain represented the average layer strain.

To calculate the total rut depth resulting from all layers, it is essential to calculate the strain in the sub-layers until the strain is no longer detectable. Based on the assumption that there is no deformation beyond a certain depth in the subgrade, the subgrade was divided into six 40-inch layers. Figure 5 shows the locations for the calculation of vertical compressive strains, and the corresponding strain values for 5 different SPS-1 sections caused by one standard 18-kip single axle. As shown in the figure the strain at the middle of the sixth subgrade layer has a very small value, as expected.

Backcalculation of Permanent Deformation Parameters (PDPs)

The backcalculation was performed based on three layers, AC, base, and subgrade. Each layer has two PDPs (α and μ); therefore a total of six parameters need to be backcalculated for each SPS-1 section. The parameter α represents the rate of decrease in permanent deformation as the number of load applications increase (hardening/densification effect). The parameter μ represents the constant of proportionality between plastic and elastic strains. As shown in equation 1, the number of load repetitions (n) is raised to the power $-\alpha$, therefore α is site-specific and has to be backcalculated by changing the number of load repetitions (i.e. using time series rutting data for each section). Rutting can be predicted by using seed values for α and μ, such as those provided in Table 3. A set of six PDPs were backcalculated for each pavement section using Microsoft Excel "Solver," by minimizing the Root Mean Square (RMS) difference between the measured and predicted rut values, as shown in Figure 6 (a).

A good agreement (small RMS) between measured and predicted rutting can be achieved; however the solution is not unique. In other words, the backcalculated parameters are dependent on the seed values. This is due to the fact that various possible distributions of rutting among the pavement layers can still lead to a similar match

for the total surface rutting. Table 3 shows the backcalculation example of PDPs for section 1-0105 using different seed values.

The most logical way to solve this problem involves knowing the rut percentage within each pavement layer, such that only two parameters can be calculated at one time. There are several ways to determine the percent rutting for each pavement layer:

- Assume the percent rutting within each pavement layer based on other studies. However these percentages are section-specific and depend on the pavement material properties, load, and climatic conditions. Therefore, it is not suitable to generalize this assumption for different pavement sections,
- Cut trenches and measure the rutting contribution from each layer. However, the inconsistency of the pavement layer thicknesses along with the noise caused by the erratic sub-layer boundary make the measurement of layer contribution difficult to determine (*14*).
- Install Linear Variable Differential Transformers (LVDTs) (e.g., a device such as the Multi-Depth Deflectometer, MDD). However, these instruments are very expensive and not suitable for long-term investigation due to durability issues (*18, 19*).
- Measure the transverse surface profile of the pavement, and estimate the contribution of each pavement layer according to the criteria described above. This can be done using non-destructive tests and can be easily monitored over time while the pavement is in-service. The LTPP database includes transverse surface profile data for all SPS-1 sections as part of the monitoring data. In addition, agencies are increasingly collecting transverse surface profiles instead of measuring only the maximum rut depth. This last method was used in the analysis.

Constraints on Backcalculation PDPs

While determining the percentage of rutting within each layer is essential for backcalculating the most likely set of PDPs, there is still the need to set lower and upper boundaries on the values of α and μ. Investigating the VESYS rutting model (equation 4) showed that α represents the rate (progression) of permanent deformation and operates within the exponent of the number of load applications as $(1-\alpha)$. Increasing the number of load applications will increase the rutting rate, meaning the exponent must be a positive value. So α is constrained to a range of values between 0 and 1. Lower values of α indicate higher rutting rates, and vice versa. The parameter μ represents the constant of proportionality between plastic and elastic strains in equation 4. Since rut depth is defined as a positive value, the value of μ has to be positive. Low values of μ indicate low initial rutting while higher μ values (>1) indicate premature rutting. These constraints were taken into consideration in the optimization procedure that involved choosing seed values from the transverse surface profiles.

Procedure for Determining Most Likely Solution of Backcalculated PDPs

As discussed above, the problem of parameter uniqueness can be dealt with by combining backcalculation strategies with transverse surface profile analysis. This combination of procedures overcomes the uniqueness problem for the backcalculation of the PDPs by limiting the number of realistic candidates. Referring to the example shown in table 3, the first ten solutions used the same seed values for all six parameters, while the remaining solutions have different seed values (according to results from previous research, see Table 1) for each parameter. The RMS values, after the second solution, were very small (less than 1%) and close to each other, indicating good agreement between the measured and predicted rut depth. However, each solution gives different rut percentages for each pavement layer. The question now is which solution is closest to the actual pavement behavior? This can be achieved by applying the following steps:

- Backcalculate the parameters using different typical seed values (see Table 2).
- For each solution calculate the RMS error and the percent rutting from each layer, as shown in Table 2. Since the RMS error is minimized when there is a good match with field measurement, solutions 1and 2 are excluded because they have higher RMS values.
- Assume that each layer will share some portion of the total rutting, unless premature rutting occurred due to construction-related issues. Based on this assumption, one can exclude solutions 3 through 11 since they have negligible detected rutting in at least one layer.
- Apply *White's* criteria (*2*) for available transverse surface profiles at different times (with more consideration for the latest available data) and point locations within the pavement section to determine

where the rutting originated. Figure 3 (d) shows the latest transverse surface profile for section 1-0105 at one point location. The shape suggests that the rutting originated in both AC and base layers.

- To further verify this initial visual assessment, the frequency of layer failure over 9 years along the 11 point locations (making a total of 99 surface profiles available for analysis) showed that 56, 37 and 3 transverse profiles experienced AC , base and subgrade layer failure, respectively. White's criteria failed to recognize any failed layer for 3 transverse profiles. Based on this, the most likely solutions are 13 and 14. However, for solution 14 some α and μ-values are outside the common range. Solution 13 satisfies all criteria, and can therefore be considered as the most likely solution for the permanent deformation parameters.

This same procedure was applied to the surface profiles for all sections in order to backcalculate the unique permanent deformation parameters; out of 120 three-layer sections, 109 sections (91%) had a most likely solution. In the remaining 11 sections, rutting measurements were too low for layer identification.

RESULTS

By applying the above procedures to distinguish the most likely solution, the backcalculated PDPs and the rutting contribution of each pavement layer were determined for all (109) sections. Figure 6 (b) shows the predicted versus actual rut depths at different ages for the 109 sections.

Excluding the sections that have:

- $\mu > 1$ which represents high initial rutting (premature rutting),
- $\alpha = 0.99$ which represents no progression of rutting with time because the majority of the rutting occurred at the initial stage,
- 100% of the rutting in the AC layer, in order to eliminate any rut failure due to specific material problems within the AC layer,

the number of sections with normal structural rutting reduced from 109 to 43 sections. Though this is a significant decrease in the amount of sections used, those that exhibit premature rutting are outside the scope of this study. Premature rutting is caused by site-specific issues during construction (e.g. asphalt mix, drainage, etc.) and are therefore not valuable for the process of understanding normal rutting behavior that extends beyond site-specific factors. The distribution of α and μ for both categories are shown in Figures 7 and 8, respectively. These figures show that excluding the abnormal sections, α-values become normally distributed. On the other hand, μ-values showed either uniform or lognormal distribution even after excluding the abnormal sections.

Comparison with Previous Results

There were several trials in the past to backcalculate the permanent deformation parameters, some of them from field data and the others from ALF. The first study predicted overall average parameters for GPS-1 sections and was not based on time series rutting data to predict the parameters for each section (*8*). Other researchers used ALF (FHWA and TxMLS) data to backcalculate the permanent deformation parameters. Figure 9 (a) shows comparisons of the average predicted PDPs from this study with those from previous studies. A good agreement exists between this study's SPS-1 predicted parameters with those of the ALF studies especially for the α values.

By establishing these PDPs for each section, the layer contribution to surface rutting was calculated using the VESYS rutting model. The results from the above developed procedure for predicting the rut percentages from each layer was compared with the measured rut depths from previous studies (AASHO and ALFs). Figure 9 (b) shows the average rut percentage of the normal behavior group (43 sections) together with those from AASHO and ALF tests. The results showed a good agreement between the predicted rutting percentages for the SPS-1 sections and the ALF-TxMLS (*19*). It should be noted that trenching was used in that study to determine the contribution to rutting from the various layers.

Finally, it should be noted that the variation in α- and μ-values presented here is due to the wide range of material properties, structural designs and climatic conditions of the SPS-1 sites. The population of backcalculated PDPs from this analysis was regressed against pavement material and structural parameters as well as climatic factors for the purpose of developing prediction models for the PDPs of various pavement layers (*20, 21*).

CONCLUSION

In this paper, time series of rut data from 109 in-service pavement sections in LTPP, SPS-1 experiment were used to predict the permanent deformation parameters for the VESYS mechanistic-empirical rut model. This was accomplished by matching the rut performance curves versus time for each section using a commercially available iterative solver. To insure uniqueness of the PDPs for a given section, the transverse surface profiles were used to match the most likely contributions by layer according to the criteria proposed in NCHRP report 468.

The range of α-values for AC, base, and subgrade layers were 0.20 to 0.90, 0.39 to 0.98, and 0.47 to 0.99, respectively. The ranges of μ-values were wider and varied from 0.01 to 1.06, 0.01 to 0.77, and 0.01 to 0.57 for the AC, base, and subgrade layers, respectively. The variation in α- and μ-values presented here is due to the wide range of material properties, structural designs and climatic conditions of the SPS-1 sites. Regression analysis should be used to explain this variation. On average, the contribution to the total surface rutting from the various pavement layers was as follows: 57 % from the AC layer, 27 % from the base layer, and 16 % from the subgrade. These results confirm that the contribution to the total rutting from AC and base layers are important and need to be included in any mechanistic-empirical design procedure.

ACKNOWLEDGEMENT

The research in this study was funded by the Michigan Department of Transportation (MDOT). The project manager is Mr. Michael Eacker.

DISCLAIMER

MDOT assumes no liability for the contents of this paper and use thereof. The contents of this paper reflect the views and opinions of the authors who are responsible for the accuracy of the information presented herein. The contents do not necessarily reflect the views of MDOT and do not constitute a department standard, specification or regulation.

REFERENCES

1. Chatti, K., N. Buch, S. W. Haider, A. Pulipaka, R. W. Lyles, D. Gilliland, and P. Desaraju. *Influence of Design and Construction Features on the Response and Performance of New Flexible and Rigid Pavements*, NCHRP., Washington DC. NCHRP Project 20-50 (10/16), NCHRP Web Document 74, http://www4.nationalacademies.org/trb/onlinepubs.nsf/web/nchrp_web_documents., 2005.
2. White, T. D., E. H. John, J. T. H. Adam, and F. Hongbing. *Contribution of Pavement Structural Layers to Rutting of Hot Mix Asphalt Pavements*, NCHRP, Washington, DC. Report 468, 2002.
3. Shook, J. F., F. N. Finn, M. W. Witczak, and C. L. Monismith. Thickness Design of Asphalt Pavement - The Asphalt Institute Method, presented at Proceedings, *5th International Conference on the Structural Design of Asphalt Pavement*, 1982, pp. 17-44.
4. Claussen, A. I. M., J. M. Edwareds, P. Sommer, and P. Uge. Asphalt Pavement Design -The Shell Method, presented at *Proceedings, 4th International Conference on the Structural Design of Asphalt Pavement*, 1977, pp. 39-74.
5. Ullidtz, P. *Pavement Analysis*. Elsevier, 1987, page 167.
6. Kim, H. B. *Framework for Incorporating Rutting Prediction Model in the Reliability-based Design of Flexible Pavements*, Ph.D. Dissertation, Civil and Environmental Engineering Department, Michigan State University, East Lansing, MI, 1999.
7. Moavenzadeh, F., J. E. Soussou, H. K. Findakly, and B. Brademeyer. *Synthesis for rational design of flexible pavement*, Federal Highway Administration *FH 11-776*, 1974.
8. Ali, H. A., S. D. Tayabji, and F. L. Torre. Calibration of Mechanistic-Empirical Rutting Model for In-service Pavements. In *Transportation Research Record: Journal of Transportation Research Board*, No.1629, TRB, National Research Council, Washington, D.C., 1998, pp.159-168.
9. Ali, H. A. and S. D. Tayabji. Using Transverse Profile Data to Compute Plastic Deformation Parameters for Asphalt Concrete Pavements. In *Transportation Research Record: Journal of Transportation Research Board*, No.1716, TRB, National Research Council, Washington, D.C., 2000, pp.89-97.

10. Kenis, W. and W. Wang. Calibrating Mechanistic Flexible Pavement Rutting Model from Full Scale Accelerating Tests, presented at *8th International conference on asphalt pavement*, Seattle, Washington, 1997, pp. 663-672.

11. Bonaquist, R. F. *Development and Application of a Comprehensive Constitutive Model for Granular Materials in Flexible Pavement Structures*," Ph. D. thesis, University of Maryland at Collage park, 1996.

12. NCHRP[1-37A]. *Guide for Mechanistic-Empirical Design of New and Rehabilitated Pavement Structures*, ARA Inc., ERES Consultants Division, Champaign, IL, Final Draft Report, March 2004.

13. Harvey, J. and L. Popescu. *Rutting of Caltrans Asphalt Concrete and Asphalt- Rubber Hot Mix Under Different Wheels, Tires and Temperatures - Accelerated Pavement Testing Evaluation*, Report Prepared for California Department of Transportation, 2000.

14. Chen, D. H., B. John, S. Tom, F. L. Deng, and F. Z. Forensic Evaluation of Premature Failures of Texas Specific Pavement Study-1 Sections, *Journal of Performance and Constructed Facilities*, vol. 17, 2003, pp. 67-74.

15. Simpson, A. L., J. F. D., and W. O. Hadley. Rutting Analysis from a Different Perspective. In *Transportation Research Record: Journal of Transportation Research Board,* No.1473, TRB, National Research Council, Washington, D.C., 1995, pp.9-16.

16. Schorsch, M. R. *Determining the Causes of Top-down Cracks in Bituminous Pavements*, Masters Thesis, Civil and Environmental Engineering Department, Michigan State University, East Lansing, MI, 2003.

17. Park, D.-Y. *Effect of Temperature and Loading Time on the Stiffness Properties of HMAC in Flexible Pavement*, Ph.D. Dissertation, Civil and Environmental Engineering Department, Michigan State University, East Lansing, MI, 2000.

18. Huang, Y. H. *Pavement Analysis and Design.* Pearson Prentice Hall, 2004, page 460.

19. Zhou, F. and T. Scullion, "*VESYS5 rutting model calibrations with local accelerated pavement test data and associated implementation*," Report No. FHWA/TX-03/9-1502-01-2, 2002.

20. Salama, H. and K. Chatti, and S. Haider "Calibration of Mechanistic-Empirical Rutting Model Using In-service Pavement Data from the SPS-1 Experiment" accepted for presentation at Transportation Research Board meeting, 85th Annual Meeting, January 2006.

21. Salama, H. Kamal. *Effect of heavy multiple axle trucks on flexible pavement rutting*, Ph. D. Dissertation, Civil and Environmental Engineering, Michigan State University, East Lansing, Michigan, 2005.

LIST OF TABLES

LIST OF TABLES

Table 1 Permanent deformation parameters *(8, 9, 10, 11)*

Calibration	Pavement layer	μ	α
LTPP (Ali *et al*., 1998)	AC	0.701	0.7
	Base	0.442	0.537
	Subbase	0.333	0.451
	Subgrade	0.021	0.752
Transverse profile (Ali and Tayabji,2000)	AC	0.000103	0.1
	Base	1.163	0.95
	Subgrade	0.0008	0.644
APT (Kenis and Wang, 1997)	AC	0.6 to 1.0	0.5 to 0.75
	Base	0.3 to 0.5	0.64 to 0.75
	Subgrade	0.01 to 0.04	0.75
APT (Bonaquist, 1996)	Asphalt concrete	0.1 to 0.5	0.45 to 0.9
	Granular base/subbase	0.1 to 0.4	0.85 to 0.95
	Sandy soil	0.05 to 0.1	0.8 to 0.95
	Clay soil	0.05 to 0.1	0.6 to 0.9

Table 2 Backcalculation of PDPs using different seed values for section 1-0105

Solution #	Seed parameter	μ_{AC}	μ_{Base}	μ_{SG}	α_{AC}	α_{Base}	α_{SG}	RMS%	AC rut %	Base rut %	SG rut %
1	0.01	0.010	0.011	0.010	0.346	0.363	0.999	7.860	27%	73%	0%
2	0.1	0.014	0.015	0.011	0.297	0.469	0.646	7.660	68%	26%	6%
3	0.2	0.010	0.113	0.081	0.681	0.544	0.693	1.055	0%	74%	25%
4	0.3	0.303	0.282	0.295	0.597	0.632	0.999	0.713	35%	65%	0%
5	0.4	0.368	0.356	0.412	0.670	0.633	0.999	0.661	18%	82%	0%
6	0.5	0.406	0.391	0.427	0.630	0.657	0.999	0.668	32%	68%	0%
7	0.6	0.515	0.532	0.523	0.584	0.758	0.999	0.642	68%	32%	0%
8	0.7	0.559	0.320	0.010	0.723	0.622	0.842	0.656	16%	84%	1%
9	0.8	0.024	0.010	0.448	0.346	0.999	0.982	0.499	60%	0%	40%
10	0.9	0.010	0.486	0.010	0.904	0.657	0.553	0.658	0%	85%	15%
11	Lower Limits of Kenis and Wang[10]	0.571	0.185	0.012	0.584	0.688	0.830	0.761	76%	23%	1%
12	Middle limits of Kenis and Wang	0.480	0.199	0.056	0.636	0.609	0.983	0.639	35%	60%	5%
13	Upper limits of Kenis and Wang	0.539	0.301	0.015	0.605	0.680	0.732	0.657	56%	41%	3%
14	Lower Limits of Bonaquist[20]	0.044	1.582	0.010	0.411	0.838	0.631	0.564	48%	46%	6%
15	Middle limits of Bonaquist	0.218	0.146	0.154	0.583	0.769	0.667	0.671	29%	8%	63%
16	Upper limits of Bonaquist	0.679	0.015	0.134	0.967	0.988	0.619	0.639	5%	1%	94%

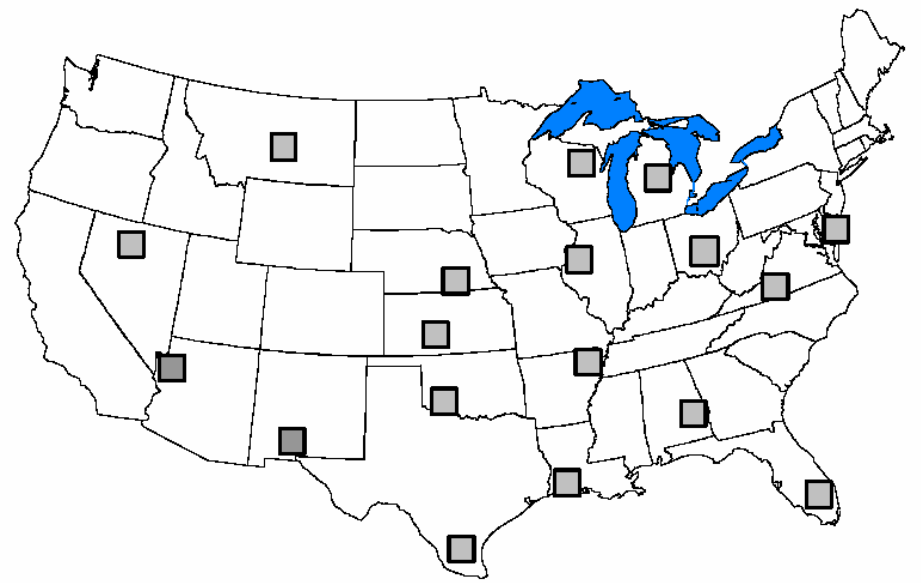

(a)

Variables	Minimum	Maximum	Average	St. dev.	COV %
HMA thickness, in	3.4	9.5	5.75	1.5	26
Base thickness, in	7.1	17.9	11.14	2.88	25.8
Rut depth, mm	3	30	8.62	5.31	61.6
KESAL/year	113	524	279	126	45.2
Age, year	0.83	10.2	6.5	2.34	36
FI*, ^{o}C-day	0	988	226	276	121.7
AARF**, mm	221	1539	846	402	47.5

* Freezing index
** Average annual rain fall
1 inch = 2.54 cm

(b)

Figure 1 SPS-1experiment: (a) Location, (b) Descriptive statistics for the experimental factors

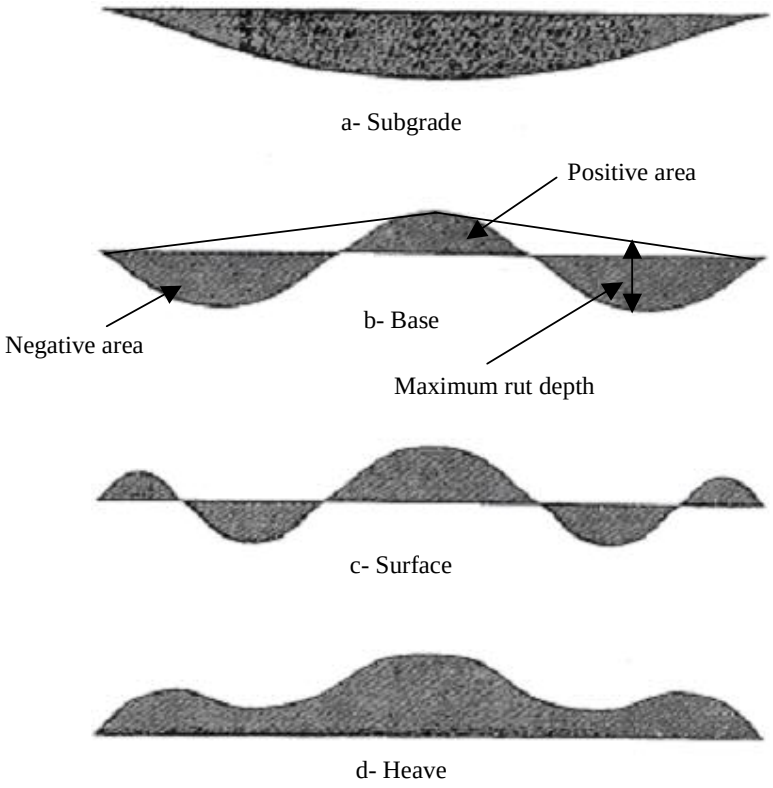

Figure 2 Transverse surface profile for various rut mechanism (*1, 13*)

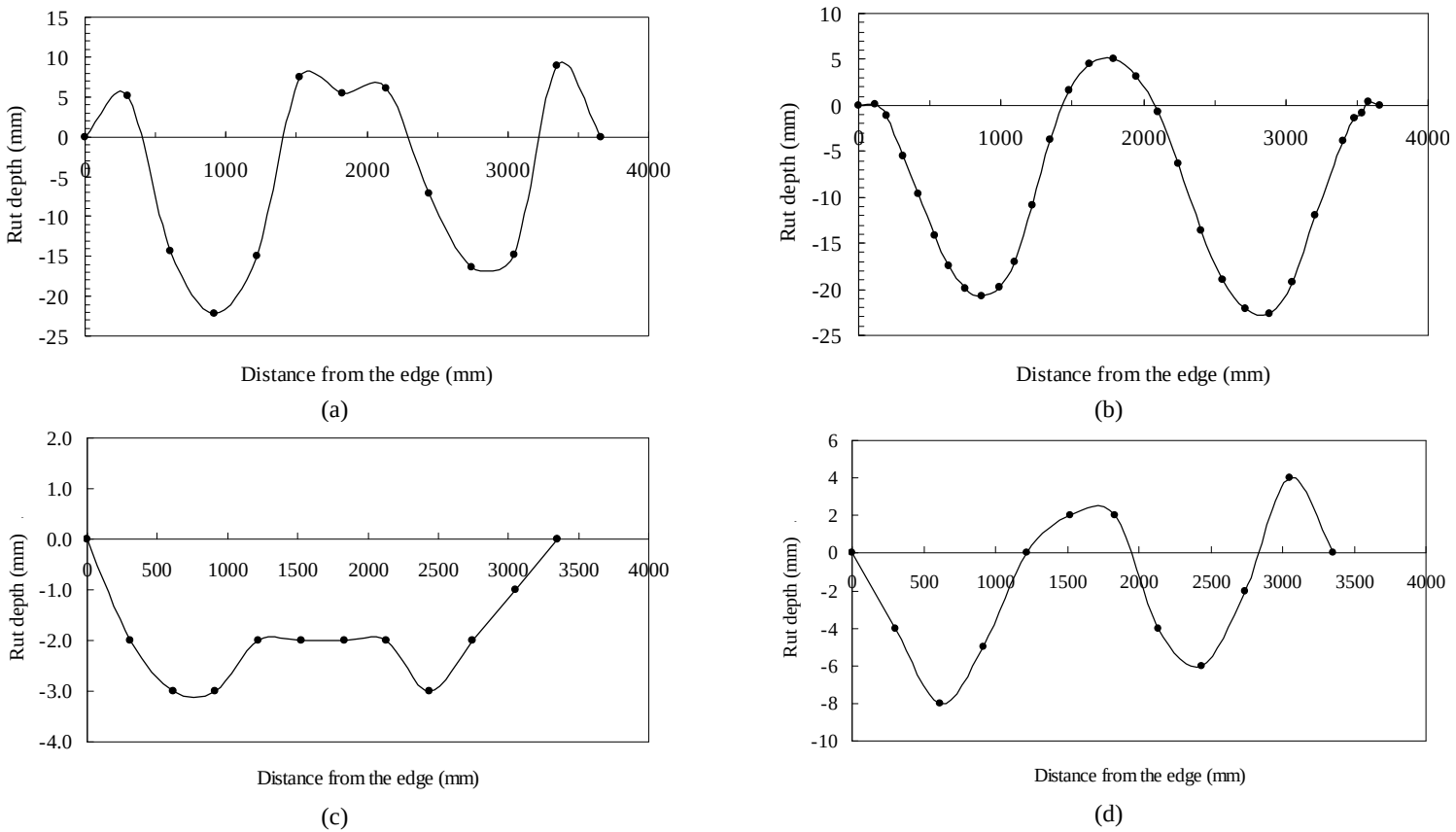

Figure 3 Different shape of transversal profiles: (a) AC layer failure (Section 31-0113), (b) base failures (Section 20-0102), and (c) subgrade rutting (Section 32-0110), (d) Transverse profile section 1-0105

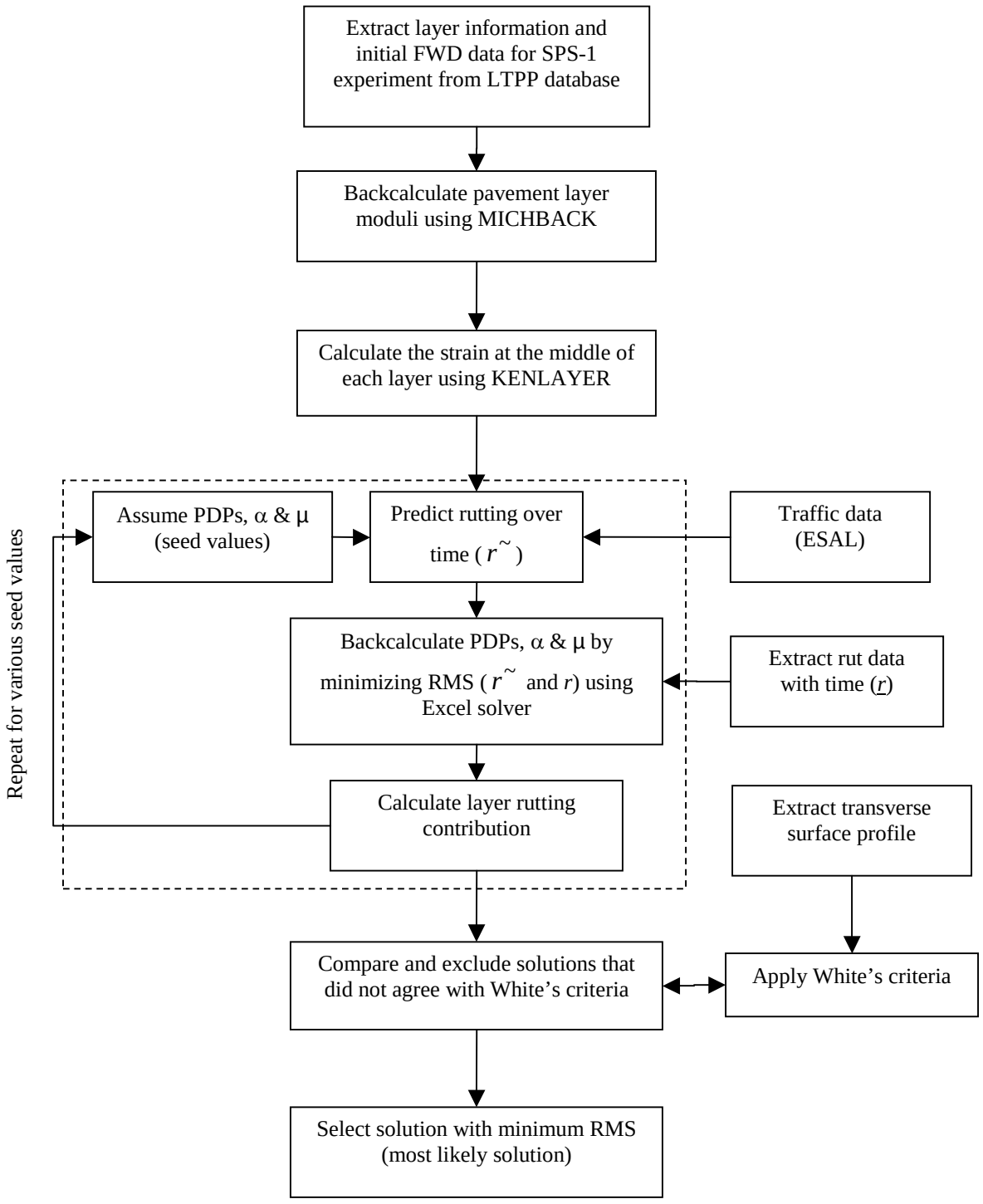

Figure 4 Flow chart of calibration of mechanistic-empirical rutting model (VESYS) using SPS-1 experiment

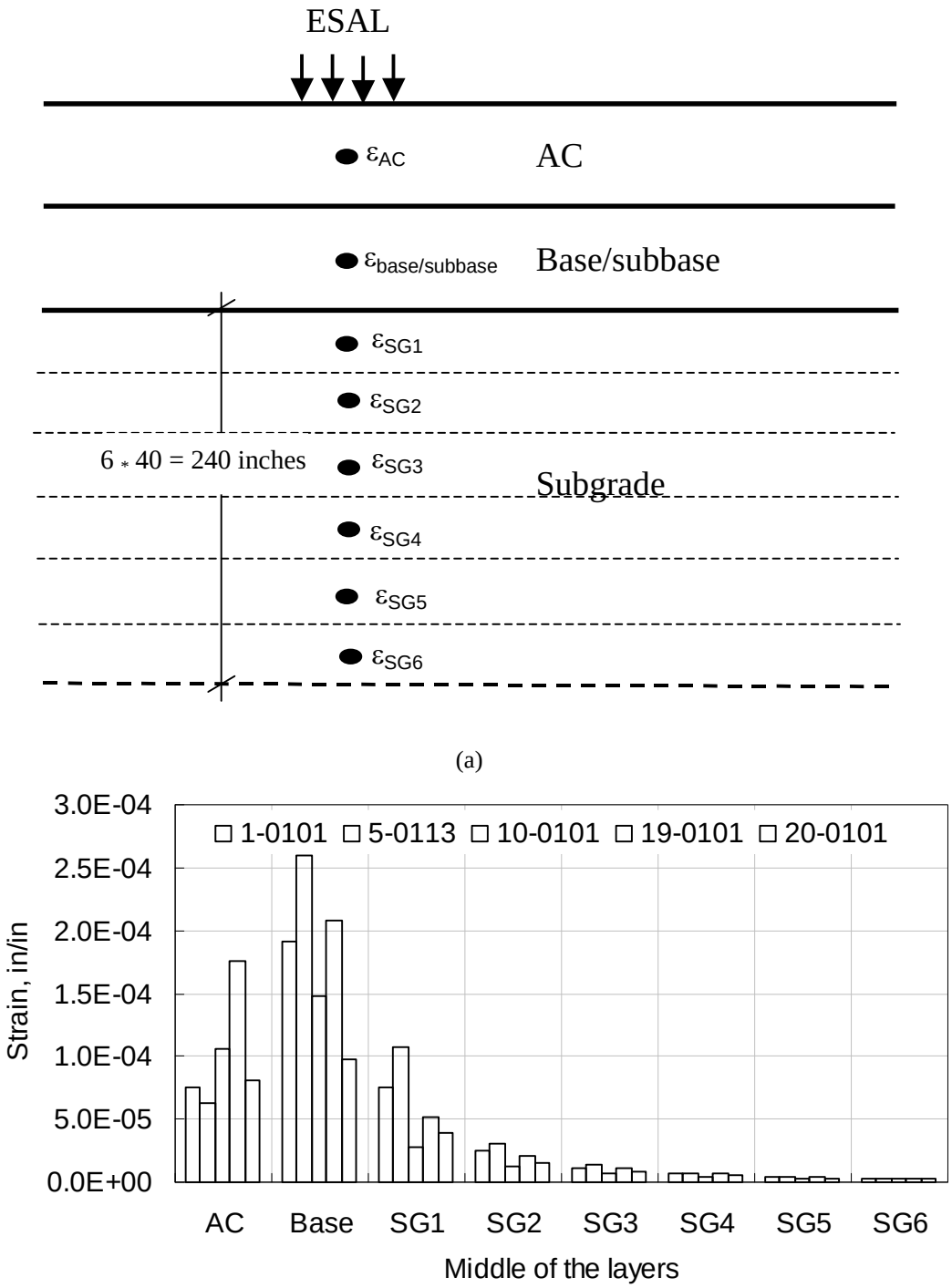

Figure 5 Forward analysis: (a) Division of the subgrade layer into several sub-layers, (b) Strain at the middle of pavement layers for 5 different SPS-1 section

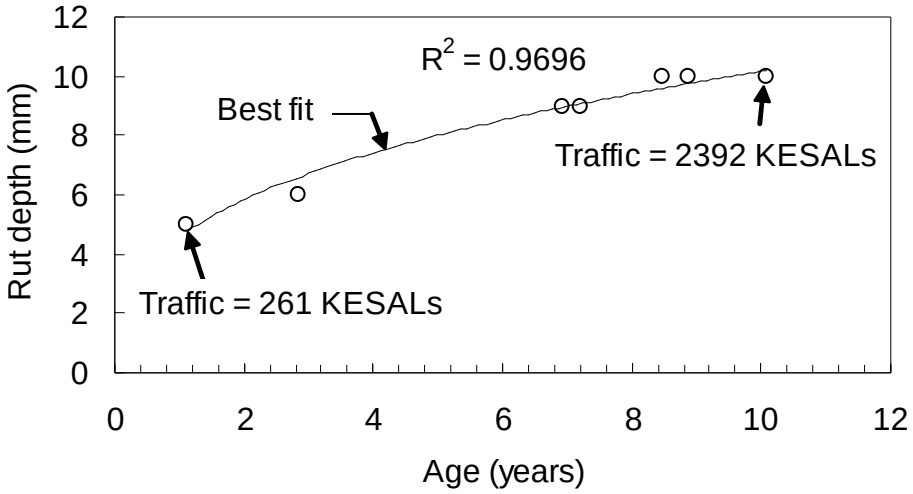

(a) Typical Time series rut data

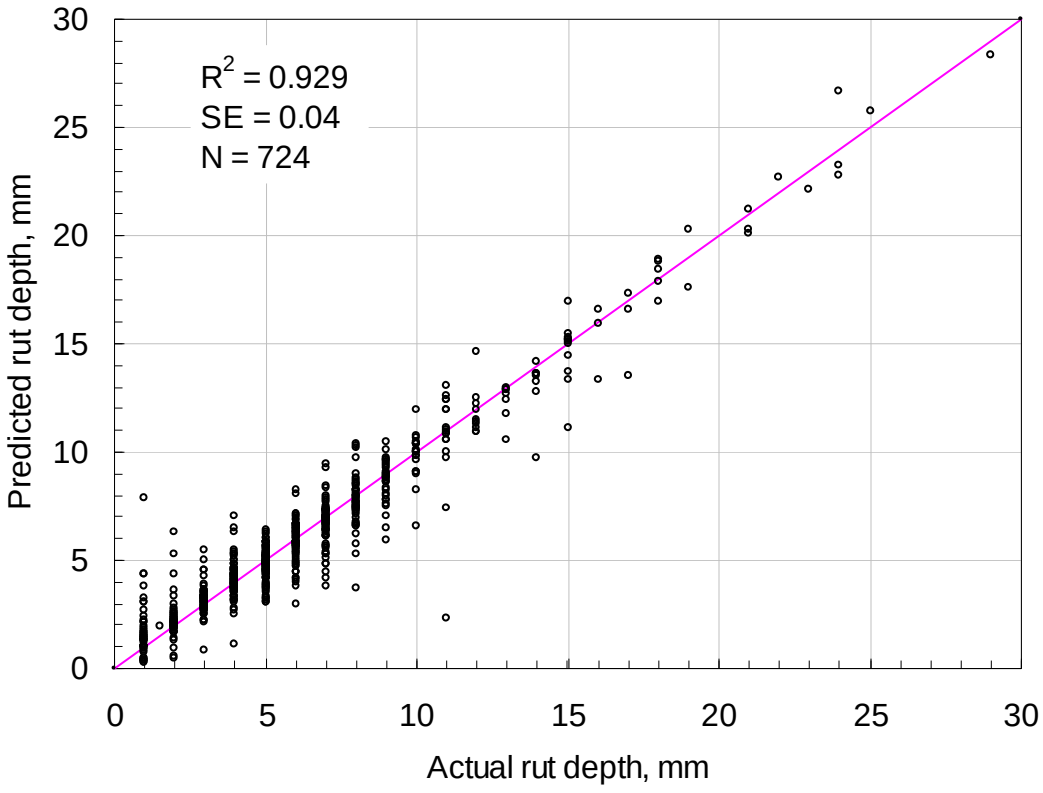

(b) Actual versus predicted rut depth

Figure 6 Time series rut data

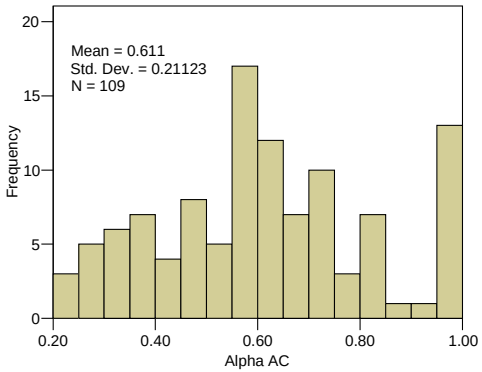

AC-layer

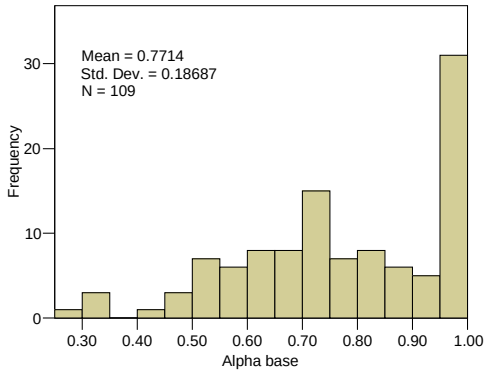

Base layer

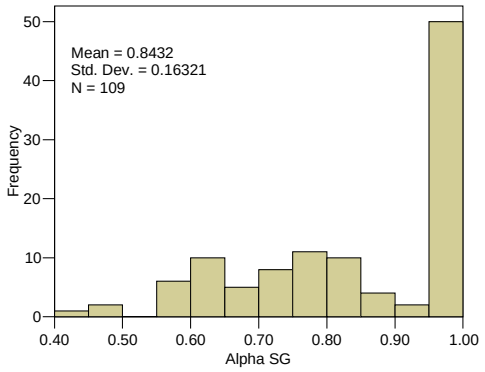

Subgrade

(a) data from all sections

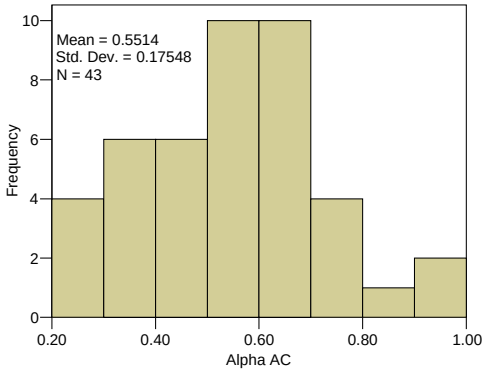

AC-layer

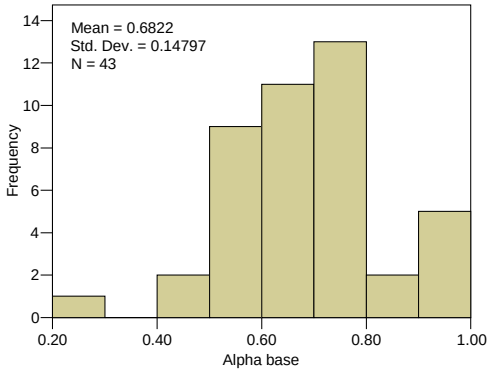

Base layer

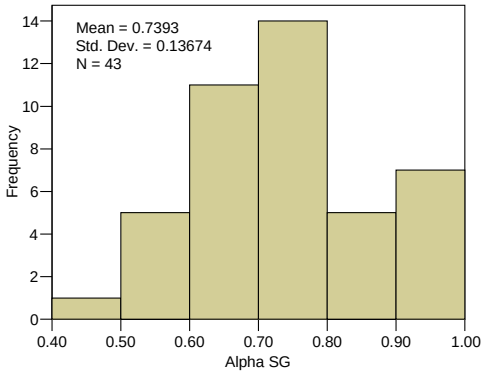

Subgrade

(b) Data from sections with structure rutting

Figure 7 α–value histograms

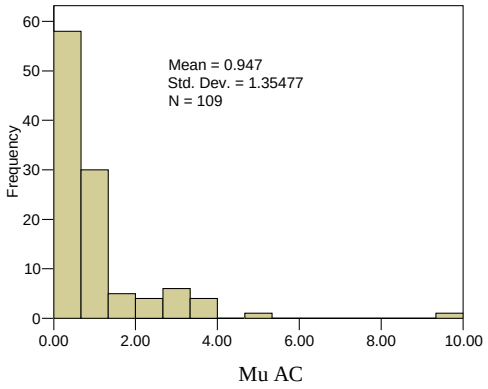

AC-layer

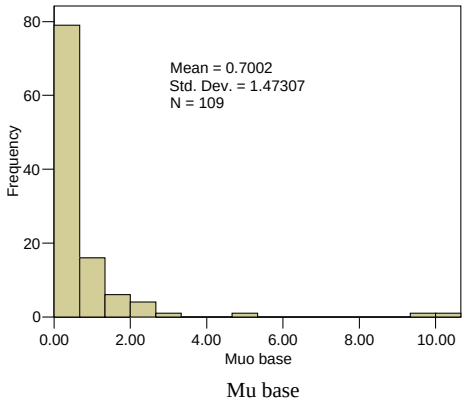

Base layer

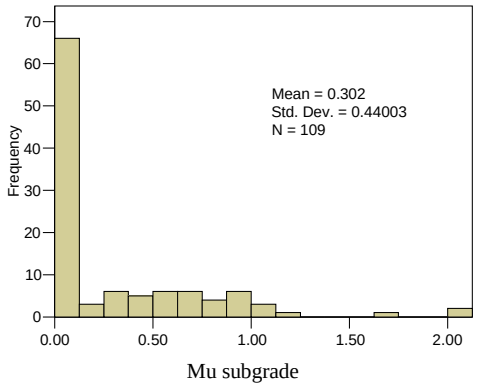

Subgrade

(a) data from all sections

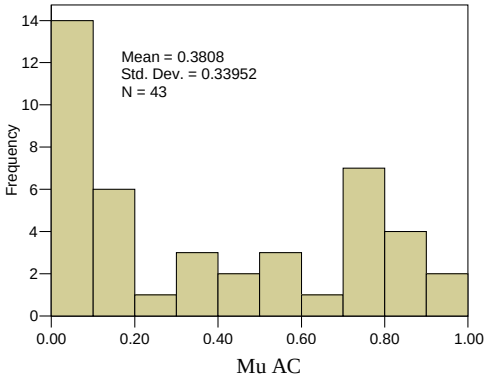

AC-layer

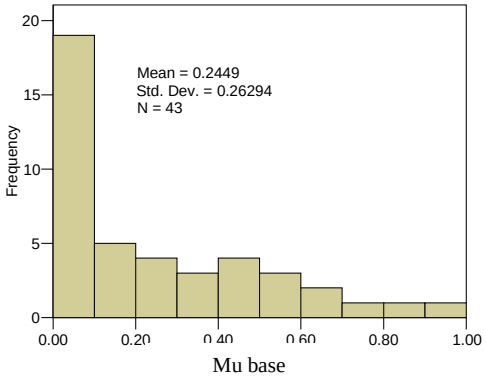

Base layer

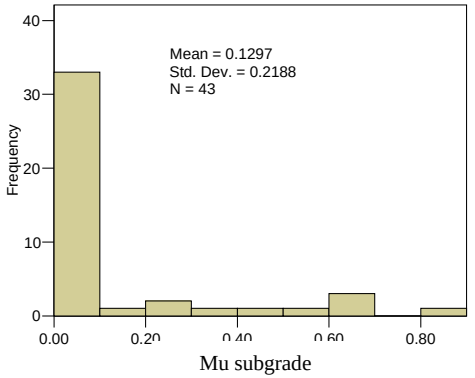

Subgrade

(b) Data from sections with structure rutting

Figure 8 μ-value histograms

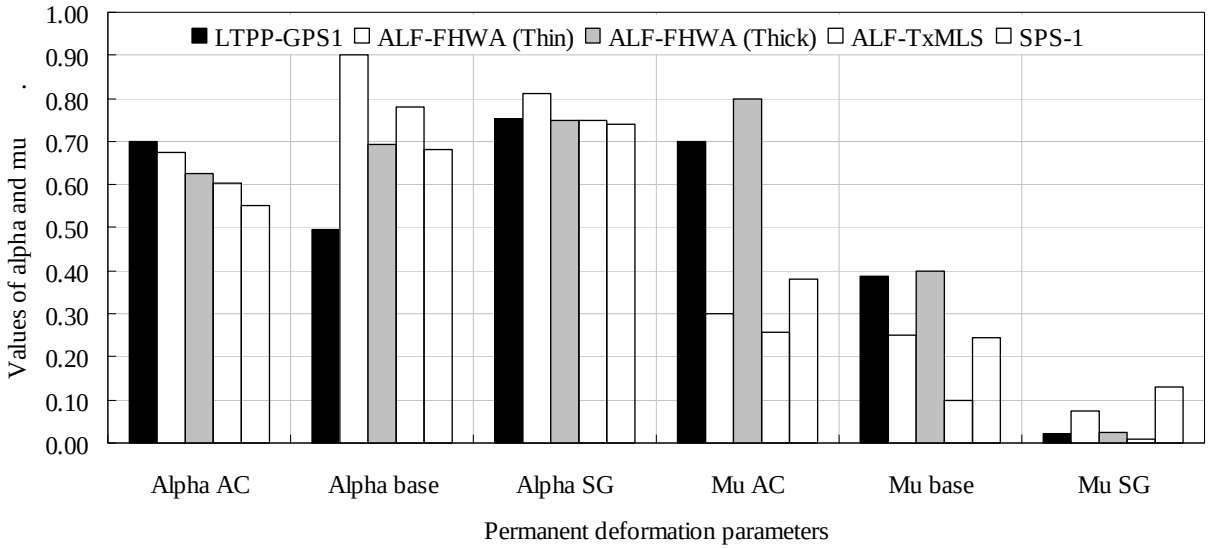

(a)

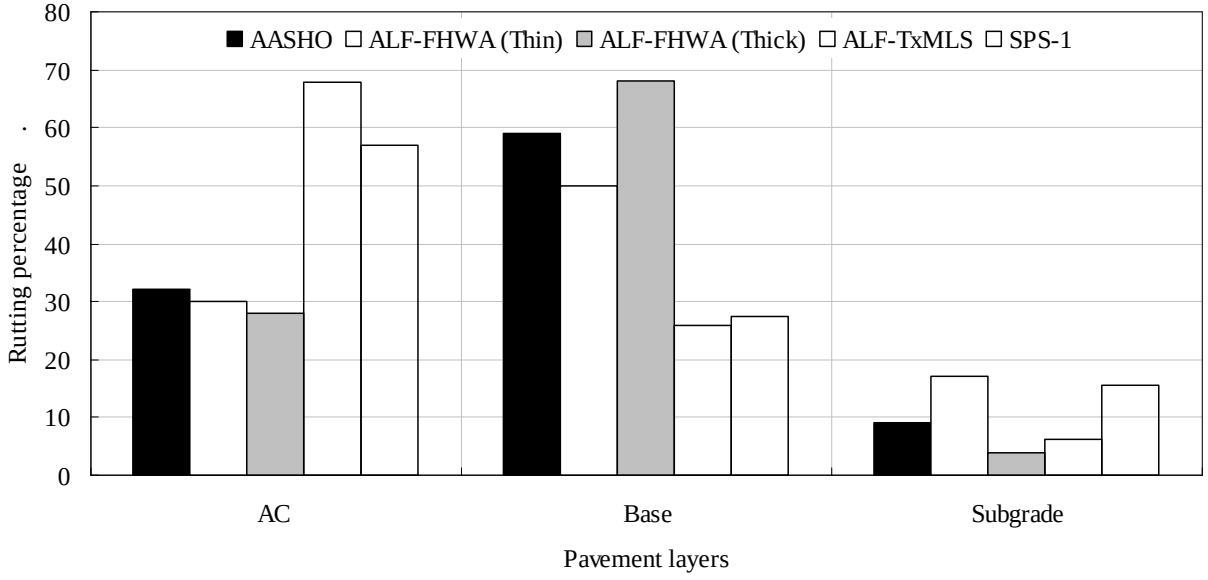

(b)

Figure 9 Comparison of SPS-1 results with previous studies: (a) permanent deformation parameters, (b) rutting contribution from individual pavement layers